



ELSEVIER

Available online at www.sciencedirect.com

SCIENCE @ DIRECT®

PHYSICS LETTERS B

Physics Letters B 571 (2003) 21–28

www.elsevier.com/locate/npe

Possibility of a two-proton halo in ^{17}Ne

R. Kanungo^a, M. Chiba^a, S. Adhikari^{b,c}, D. Fang^a, N. Iwasa^d, K. Kimura^e,
K. Maeda^d, S. Nishimura^a, Y. Ogawa^f, T. Ohnishi^a, A. Ozawa^a, C. Samanta^{b,c},
T. Suda^a, T. Suzuki^g, Q. Wang^h, C. Wu^a, Y. Yamaguchi^g, K. Yamada^a, A. Yoshida^a,
T. Zheng^a, I. Tanihata^a

^a RI Beam Science Laboratory, The Institute of Physical and Chemical Research, 2-1 Hirosawa, Wako-shi, Saitama 351-0198, Japan

^b Physics Department, Virginia Commonwealth University, West Main Street, Richmond, VA 23284, USA

^c Saha Institute of Nuclear Physics, 1/AF, Bidhannagar, Calcutta 700064, India

^d Department of Physics, Tohoku University, Miyagi 980-8578, Japan

^e Department of Electric, Electronics and Computer Engineering Nagasaki Institute of Applied Science, Nagasaki 851-0193, Japan

^f Research Center for Nuclear Physics, Osaka, Japan

^g Department of Physics, Niigata University, Niigata 950-218, Japan

^h Department of Technical Physics, Peking University, Beijing 100871, PR China

Received 5 March 2003; received in revised form 11 July 2003; accepted 15 July 2003

Editor: J.P. Schiffer

Abstract

The first measurement of the two proton removal, cross section and momentum distribution, with a Be target at 66 A MeV are reported. The momentum distribution shows a width of 168 ± 17 MeV/c (FWHM) that is much narrower than the width expected from a normal nucleus (~ 290 MeV/c). The proton removal cross-section has been determined to be 191 ± 48 mb. Analysis of present data together with interaction cross section indicates significant *s*-wave probability of the two valence protons. This suggests a two-proton halo in ^{17}Ne .

© 2003 Published by Elsevier B.V.

Keywords: ^{17}Ne ; Proton halo; Momentum distribution; Proton removal cross section; Interaction cross section; Glauber model

Over the past decade studies of unstable nuclei led to the discovery of nuclear halo structures close to neutron drip line [1]. Investigations around the proton drip line in search of such structures are however few. One-proton halo formation in ^8B , ^{27}P [2,3] has been discussed but so far there has been no conclusive evidence for a two-proton halo. The presence of the

Coulomb barrier of course is a main hindrance to the formation of a proton halo. So even if, a one-proton halo might be visualized to be formed, existence of a two-proton halo seemed to be a rare possibility.

The ^{17}Ne nucleus is an attractive candidate for search for a possible two-proton halo with its Borromean character and small two-proton separation energy $S_{2p} = 0.94$ MeV. Previous experimental studies like the measured interaction cross section systematics for the Ne isotopes and the $A = 17$ isobars suggest

E-mail address: ritu@postman.riken.go.jp (R. Kanungo).

a probable halo formation [4]. The large beta-decay asymmetry observed between ^{17}Ne and ^{17}N is also suggestive of an abnormal orbital for the valence protons in ^{17}Ne [5]. From a reaction cross section measurement at intermediate energies, Warner et al., however, concludes that a halo does not exist in ^{17}Ne [6].

Recent theoretical efforts also present a contradictory picture as a dominance of protons occupying the $1d_{5/2}$ orbital is suggested by Fortune and Sherr from a consideration of Coulomb energy [7]. The work of Millener [8] in addressing the beta decay asymmetry also reaches the same conclusion of a d -wave dominance. The possibility of a proton halo in ^{17}Ne is discussed however, from Glauber calculations with Hartree–Fock wavefunctions in Ref. [9]. A calculation based on Faddeev model wavefunctions [10,11] also suggests a two-proton halo for ^{17}Ne and predicts momentum distributions, whose measurement should confirm the existence of a two-proton halo.

The situation regarding halo formation in ^{17}Ne is thus not clear. Theoretical models of nuclear structure need to be used to interpret the observed large interaction cross section, in order to estimate the relative contribution of the s - and d -orbital occupancies of the protons and to comment on a possible halo structure. Furthermore, it must be noted that an enhancement of the interaction cross section alone does not necessarily confirm the existence of a halo. Large deformation at times, could also be reflected in large cross sections. The formation of a halo structure is confirmed only when one observes a relatively narrow momentum distribution coupled with a large interaction cross section under a consistent description of both on the same footing. The shape of the momentum distribution portrays the valence nucleon orbital and is hence a reliable probe in search of exotic structures.

In this Letter we report the first measurements of the longitudinal momentum distribution ($P_{||}$) for two-proton removal from ^{17}Ne using the newly developed time-of-flight (TOF) technique [12]. The observed momentum distribution has a narrow width compared to the Goldhaber width for an ^{15}O core. Furthermore, the few-body Glauber-model [16] analysis of the measured distribution and the two-proton removal (σ_{-2p}) as well as interaction cross sections (σ_I) taken together, suggests the valence protons to have a large probability of occupying the $2s_{1/2}$ orbital. This is

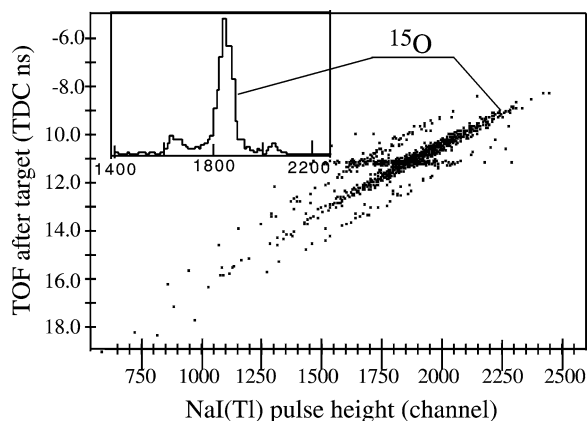


Fig. 1. Particle identification spectrum after the reaction target. The spectrum is already charge selected ($Z = 8$). The inset shows the NaI(Tl) projection of the spectrum after correcting for the TOF-E correlation.

thus suggestive of two-proton halo formation in this nucleus.

The experiment, with a $135 \text{ A MeV } ^{20}\text{Ne}$ primary beam, was performed using the RIKEN Projectile Fragment Separator (RIPS). The secondary ^{17}Ne beam with an average intensity of 120 pps and energy of 66 A MeV interacted with a 0.5 mm Be reaction target placed at the second focus, F2, (achromatic) of RIPS.

The fragments produced after the reaction target were transported to the final achromatic focus (F3), through focusing magnets. The angular acceptance of the fragments after the reaction target is $\sim \pm 32 \text{ mrad}$. It has been confirmed that there is no distortion in the shape of the momentum distribution in this method, even for nuclei with Goldhaber broadening. Two scintillators placed 5.2 m apart after the reaction target provided the TOF information of the breakup fragments. A 60 cm long ion chamber, operated with Ar gas at 1 atm , at room temperature, was used as an energy-loss (ΔE) detector after the scintillators. The total energy (E) information was obtained from a 6 cm thick NaI(Tl) detector placed further downstream.

The fragments were mass separated using the E and TOF information after the target (Fig. 1). The charge separation was achieved by using the ΔE and TOF information. The momentum of the incident ^{17}Ne nucleus could be obtained from position sensitive detectors placed at the dispersive focus (F1) of RIPS. The TOF after target provided the momentum of the

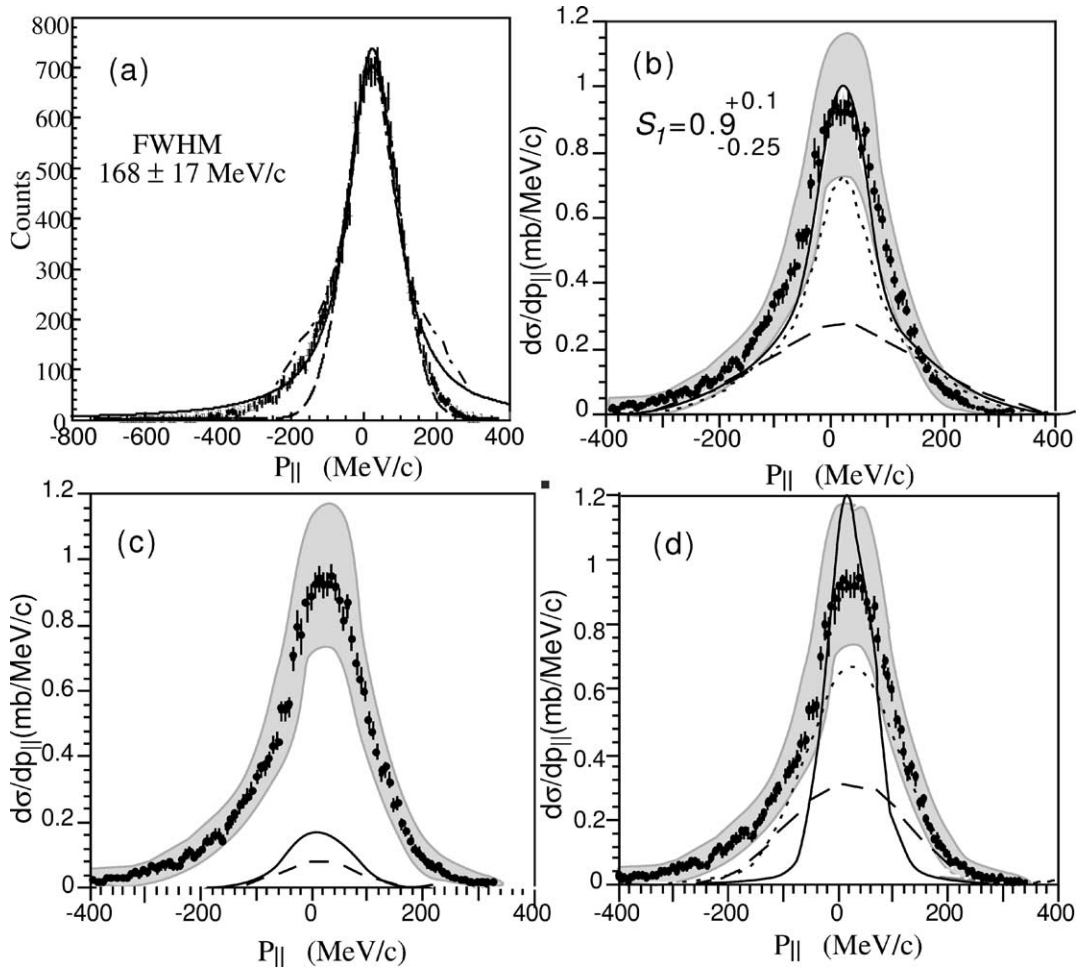


Fig. 2. The $^{17}\text{Ne} \rightarrow ^{15}\text{O}$ longitudinal momentum distribution data. The shaded regions in (b)–(d) show the uncertainty of the overall normalisation in σ_{-2p} . (a) The solid (long-dashed) lines are Lorentzian (Gaussian) fits to the data. The dash-dotted line shows the predictions of Ref. [10]. (b) The solid curve indicates the prediction of the model-1 for pure s -wave configuration of two-valence protons ($S_1 = 1$), and the long-dashed curve present that for pure d -wave configuration ($S_1 = 0$). The $S_1 = 0.9_{-0.25}^{+0.1}$ gives momentum distribution consistent with the experimental data. The short-dashed curve shows the momentum distribution that is consistent with the data with the smallest value of S_1 ($= 0.65$). (c) The lines show calculations considering model-2 (see text). (d) The lines represent results considering model-3 (see text). The solid/long-dashed/short-dashed lines represent proton emission from $s/d/p$ orbitals.

breakup fragments. The momentum resolution in the present experiment was $18.8 \text{ MeV}/c$ FWHM.

The main source of background in the $P_{||}$ distribution of $^{17}\text{Ne} \rightarrow ^{15}\text{O}$ was primarily due to ^{17}Ne reacting in the scintillator at F3. This small background was subtracted using the procedure described in Ref. [12] and also reconfirmed from subtraction with target out data. The other $Z = 8$ fragments observed in Fig. 1 are ^{14}O and ^{16}O on the left and right side of ^{15}O , respectively.

The background-subtracted momentum distribution is shown in Fig. 2 fitted by a Lorentzian (solid line) and Gaussian (long-dashed line) (Fig. 2(a)). The spectrum appears asymmetric having a low momentum tail which is expected due to multistep reactions that become important at energies under discussion. Such asymmetry has been discussed recently by Tostevin et al. [13]. The data with error bars (if connected by smooth line) has a FWHM of $168 \pm 17 \text{ MeV}/c$. The FWHM of this distribution from a

Lorentzian (Gaussian) fit is 153 ± 3 MeV/c (183 ± 2 MeV/c) which when unfolded by the system resolution yields a value of 151 ± 3 MeV/c (181 ± 2 MeV/c). The two-proton removal from the core nucleus ^{15}O shows a Goldhaber width ~ 290 MeV/c. A comparison therefore, suggests a halo formation in ^{17}Ne . The measured σ_{-2p} was 191 ± 48 mb where the large uncertainty reflects mainly the estimates of transport efficiency and the acceptance.

The ground state configuration of ^{17}Ne , is considered to be a ^{15}O core + $p + p$ structure. In this article we assume that ^{15}O core coupled to two protons either in $2s_{1/2}$ or $1d_{5/2}$ are the main configurations. The aim of this analysis is to see qualitatively the relative contributions of the $2s_{1/2}$ and $1d_{5/2}$ wavefunctions in the ground state. One can thus write the wavefunction of ^{17}Ne as $\Psi_{\text{Ne}}(\mathbf{r}) = a_1 \psi_C(\mathbf{r}) \phi_{2s_{1/2}}^{J=0}(\mathbf{r}_1, \mathbf{r}_2) + a_2 \psi_C(\mathbf{r}) \phi_{1d_{5/2}}^{J=0}(\mathbf{r}_1, \mathbf{r}_2)$, where ψ_C is the core wavefunction and $\phi(\mathbf{r}_1, \mathbf{r}_2)$ is the proton wavefunction. The densities of the ^{15}O core and the protons are individually normalised to the respective particle numbers. Thus, the two-proton spectroscopic factors, $S_1 = |a_1|^2$ and $S_2 = |a_2|^2$, satisfy the relation $S_1 + S_2 = 1$.

To interpret the $P_{||}$ distribution and the measured σ_{-2p} in a few-body Glauber model we consider three different possibilities. Firstly, ^{17}Ne is visualized as having a ^{15}O core plus two uncorrelated proton structure, where two uncorrelated protons are emitted simultaneously (model-1). Secondly, we adopt the possibility of a ^{15}O core plus a di-proton configuration and knockout of a di-proton cluster (model-2) and thirdly, we explore the possibility of two proton emission through the decay of unbound states of ^{16}F (model-3). In this model, a proton is knocked out by the collision leaving the pre-fragment (^{16}F) in unbound states. Then another proton is emitted from the excited states.

In model-1, the two protons are treated as identical, each having a separation energy (S_p) equal to half the two-proton separation energy (S_{2p}). This is a reasonable choice and has been used in Refs. [14,15] for borromean nuclei. The prediction from model-1 is shown in Fig. 2(b), where the solid line indicates $S_1 = 1$ (pure s -wave) case and the long-dashed line indicates $S_1 = 0$ case. As can be seen in the figure, $S_1 = 1.0$ is consistent with the data and $S_1 = 0$ is not. Varying the S_1 value, a consistent fit to the data is

obtained for $S_1 = 0.9_{-0.25}^{+0.1}$. In addition to the curve corresponding to the upper limit of S_1 ($= 1.0$), the curve corresponding to the lower limit of S_1 ($= 0.65$) is also shown in the figure by short-dashed curve to visualize the fitting.

Fig. 3(a) (solid line) shows the calculated values of the two-proton removal cross section in model-1. The values are also listed in Table 1. It is seen that both the momentum distribution and the σ_{-2p} are reproduced with $S_1 = 0.9_{-0.25}^{+0.1}$. In normal shell model ordering these protons should occupy the d -orbital which however yields a much wider distribution and smaller proton removal cross section that is well outside experimental errors.

In model-2, we look into the possibility of a di-proton configuration with the total angular momentum of the protons coupled to zero. Here the protons could once again either be in the s -orbital (solid line in Fig. 2(c)) or in the d -orbital (dashed line in Fig. 2(c)). Consideration of a di-proton, however, leads to a much less extended wavefunction than the former due to increased Coulomb barrier and separation energy. This results in an extremely small σ_{-2p} (Table 1). Thus, although the width of the calculated momentum distribution appears fairly consistent with the measured one, the value of cross section is far below the experimental data (Fig. 2(c)).

In model-3, we consider three different paths. (a) In the first path, one proton from the s -orbital is knocked out and results in the lowest 0^- resonance in ^{16}F which then decays to the ground state of ^{15}O by proton emission. So ^{17}Ne in this possibility can be modeled as $^{16}\text{F}^* + p$ where the effective separation energy is $S_p(^{17}\text{Ne}) = 1.479$ MeV. The proton is in $2s_{1/2}$ orbital. Here, $^{16}\text{F}^*$ acts as a core for the Glauber model calculation. This core, is described by ^{15}O (harmonic oscillator density) plus proton (in s -orbital with $S_p = S_{2p}^{17\text{Ne}}/2$). The momentum distribution in this process (Fig. 2(d), solid line) is much narrower than the data. The calculated σ_{-2p}^s is shown in Table 1.

(b) In the second path, one proton is emitted from the d -orbital and produces ^{16}F in its lowest 2^- state (424 keV), $S_p = 1.903$ MeV. Here, the $^{16}\text{F}^*$ core is described by ^{15}O (harmonic oscillator density) plus proton (in d -orbital with $S_p = S_{2p}^{17\text{Ne}}/2$). The momentum distribution from such a process is shown by the long-dashed curve in Fig. 2(d). The calculated

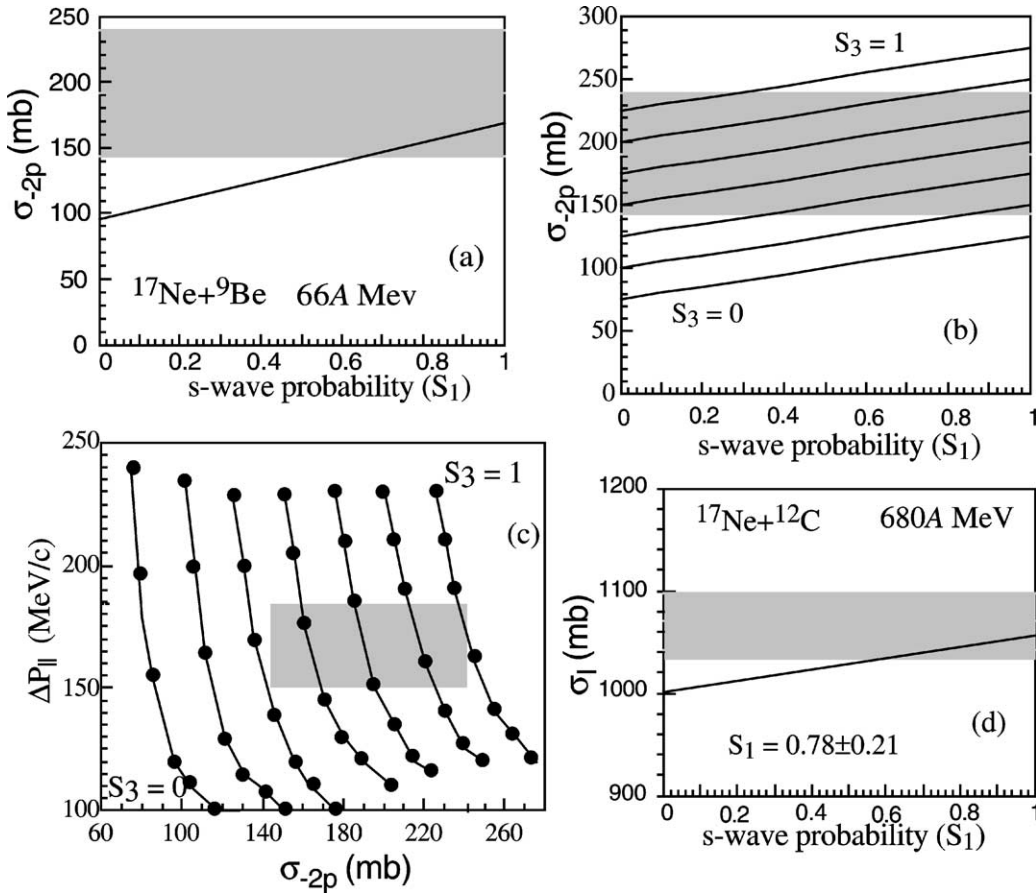


Fig. 3. (a) The shaded region is the measured two-proton removal cross section for $^{17}\text{Ne} + ^9\text{Be}$ at 66 A MeV. The solid line is the few body Glauber calculation for model-1. (b) The shaded region is as in (a). The solid lines are Glauber calculations for model-3 as explained in the text. The lines are for different values of S_3 from 0 to 1 in steps of 1/6. (c) The shaded region indicates the observed $P_{||}$ width and σ_{-2p} . The solid lines are the calculated loci for different values of S_3 . From left to right $S_3 = 0.0$ –1.0 in steps of 1/6. The dots along each locus shows values of $S_1 = 0.0, 0.1, 0.2, 0.4, 0.6, 0.8, 1.0$ from top to bottom. (d) The interaction cross section data (shaded region) shown is the weighted mean of two data from Ref. [4] for $^{17}\text{Ne} + ^{12}\text{C}$ at 680 A MeV. The solid line is a few body Glauber calculation for model-1.

cross section (σ_{-2p}^d) is shown in Table 1. It may be mentioned that this d -wave distribution shows an improved fit to the high-momentum tail of the data as compared to Fig. 2(b).

(c) In the third path we consider the emission of a proton from the $1p_{1/2}$ and $1p_{3/2}$ orbitals in the core. This leads to the 1^+ resonances at 3.758 and 4.65 MeV, respectively, in ^{16}F . Here, the $^{16}\text{F}^*$ core is described by ^{15}O (harmonic oscillator density) plus proton (in p -orbital with $S_p = S_{2p}^{17\text{Ne}}/2$). Since the excitation energies of the two 1^+ resonances considered differ only by 1 MeV, it is found that the one-proton removal cross sections from both $p_{1/2}$

and $p_{3/2}$ calculated in a core + p model are similar (~ 25 mb). In total there are 6 protons in the p -orbital therefore, the total removal cross section $\sigma_{-2p}^p = 150$ mb (Table 1). The momentum distribution from such a process is shown by the short-dashed curve in Fig. 2(d).

None of the three paths can fit the data individually. Therefore, we consider a mixing of these three paths. Since the proton removal from the core (p -wave) is not related to a separate ground state configuration as described above, the two-proton spectroscopic factor (S_3) for it can be any value ranging from 1 (100% probability of two protons emitted from $1p_{1/2}$ and

Table 1

Calculated two-proton removal and interaction cross sections for the different proton emission models. The agreement with experimental data is indicated by \circ = good agreement, Δ = fair agreement, \times = disagreement within experimental errors of Fig. 2(b)–(d)

Model	Proton orbital	σ_I (mb)	σ_{-2p} (mb)	$P_{ }$ (FWHM)
		680 A MeV	66 A MeV	66 A MeV
Data		1065 ± 32	191 ± 48	168 ± 17
Core + uncorrelated protons	<i>s</i>	$1056 \circ$	$168 \circ$	125Δ
	<i>d</i>	$1000\times$	$94\times$	$325\times$
Core + diproton	<i>s</i>	$948\times$	$30\times$	$135 \circ$
	<i>d</i>	$941\times$	$14\times$	$155 \circ$
Decay through $^{16}\text{F}^*$	<i>s</i>		125	100
	<i>d</i>		75	225
	<i>p</i>		150	210

$1p_{3/2}$ orbitals) to 0 (no emission of the core protons) independent of the factors S_1 and S_2 . Although, such factors can be calculated from a shell model, we have no experimental guidance of this factor from an inclusive measurement. We thus, consider them as parameters here.

The σ_{-2p} calculated in such a mixed emission is thus given by $\sigma_{-2p} = S_1\sigma_{-2p}^s + S_2\sigma_{-2p}^d + S_3\sigma_{-2p}^p$ where $S_1 + S_2 = 1$ and $0 \leq S_3 \leq 1.0$ as explained above. The Fig. 3(b) shows the relation between the S_1 value and σ_{-2p} . The shaded area shows the experimental value of σ_{-2p} . The different lines in Fig. 3(b) correspond to different values of S_3 . It shows that the inclusion of *p*-wave removal is necessary to explain the cross section. To obtain a consistent understanding of the width of the $P_{||}$ distribution ($\Delta P_{||}$) and σ_{-2p} under this model, we study the locus on the $\Delta P_{||}$ and σ_{-2p} plane of these calculated values in Fig. 3(c). Again the shaded area is the experimental observation. The different solid lines represent the different values of S_3 from 0 to 1.0 in steps of 1/6. It is found that only loci for $S_3 > 0.3$ (i.e., more than two protons in *p*-orbitals) overlap with the one standard deviation experimental area. Therefore, proton knockout from the deeply bound $1p_{3/2}$ orbital is necessary for explaining the observation. The *s*-wave spectroscopic factor which is consistent with the experimental region ranges from $S_1 \sim 0.5$ to 0.2.

It should be mentioned here that the results discussed with model-3 would change significantly if ^{16}F core density is larger than our estimation. In such case, the calculated proton removal cross sections would be smaller and the momentum distributions slightly

wider. In the limit of unbound ^{16}F having a density with root-mean-square radius larger than that of ^{17}Ne , the process of proton emission by model-3 will not exist. In this context, it may be useful to re-investigate the two-neutron removal studies from neutron rich nuclei, e.g., ^{11}Li , ^{17}B within the framework of neutron evaporation.

A summary for analysis of $P_{||}$ and σ_{-2p} within the above three models, thus gives two possibilities. As one solution, we have a consistent understanding of the data with a strong probability of the two protons occupying the $2s_{1/2}$ orbital, in model-1. The other alternative, seems to be the process of proton evaporation (model-3) which suggest that protons could have about 50–20% probability of residing in the $2s_{1/2}$ orbital and fair amount of *p*-wave knockout contribution.

As mentioned at the onset, to confirm the existence of a halo, the Heisenberg's uncertainty principle must be satisfied. So a consistent understanding of the structure should be achieved from both the momentum distribution and the interaction cross section measurements. Thus, in the next step, we investigate the radial extent of ^{17}Ne from the measured interaction cross section (σ_I) [4].

The interaction cross section reflects on the total size of the nucleus and thus, it is best described by the most suitable model available for the nucleus. Since, we have two identical valence protons, the models 1 and 2 (with $^{17}\text{Ne} = ^{15}\text{O} + p + p$) are appropriate to describe σ_I . Model-3 differs from the other two in the mechanism of proton emission only and thus has no relevance to a separate interpretation of σ_I . In particular, the value of S_3 does not contribute to the

interaction cross section. The knockout process from p -wave is a single proton removal from the core and thus is included in the core breakup process in the interaction cross section calculations. Therefore, only S_1 contributes to change of interaction cross section. The prediction of interaction cross section is thus considered to be same as those of model-1.

We thus analyse the σ_I ($^{17}\text{Ne} + ^{12}\text{C}$ at 680 A MeV) in the models 1 and 2. The core ^{15}O is considered to have a harmonic oscillator density, that includes the protons in the p -orbitals. The width of the harmonic oscillator is adjusted to reproduce the experimental σ_I [4] for $^{15}\text{O} + ^{12}\text{C}$. The valence protons are considered to be either in the $2s_{1/2}$ or the $1d_{5/2}$ orbitals, as explained above.

The results are shown in Table 1 and Fig. 3(d). The data can be explained in model-1 by $S_1 = 0.78 \pm 0.21$. Model-2 gives very small cross section compared with the data (Table 1). The value of S_1 (0.5–0.2), required for fragmentation in model-3, does not agree with the measured σ_I .

Thus, a consistent description of $P_{||}$, σ_{-2p} and σ_I can be obtained only in model-1 (uncorrelated two proton emission) with $S_1 = 0.9_{-0.25}^{+0.1}$. The root-mean-square (rms) radius of ^{17}Ne from such a picture is $\sim 2.75 \pm 0.03$ fm while that of the ^{15}O core is ~ 2.42 fm. The rms radius of the halo proton wavefunction is $\sim 4.55 \pm 0.15$ fm. It should be mentioned here that the observed width of momentum distribution is consistent with the predictions of a proton halo in Ref. [10] (Fig. 2(a); dash-dotted line).

This is unlike the case of the mirror nucleus $^{17}_7\text{N}$ where magnetic moment measurements [17] favor the two neutrons to occupy predominantly the $1d_{5/2}$ orbital coupled to $J^\pi = 0^+$, with a small admixture of two neutrons occupying $2s_{1/2}$ orbital. Furthermore, the necessity of two neutrons coupled to $J^\pi = 2^+$ in $^{17}_7\text{N}$ is found to be important for explaining the observed magnetic moment. The interaction cross section data [4] of ^{17}N is also much smaller and both the momentum distribution data as well as the one neutron removal cross section data can be interpreted as valence neutrons dominantly occupying the $1d_{5/2}$ orbital [18].

In conclusion, the first measurement of two-proton removal momentum distribution and cross section are presented in this Letter. The data shows a narrow momentum width compared to the core ^{15}O , thereby

indicating the possible presence of the first two-proton halo.

The present data together with existing interaction cross section data for ^{17}Ne are analyzed in the framework of few-body Glauber model. All the data taken together provide a consistent understanding with a ^{15}O -plus-two uncorrelated proton picture of ^{17}Ne . Within the present models, a large s -wave occupancy of the valence protons is suggested. The extent of the halo is of course somewhat hindered compared to neutron-rich cases. Quite different ground-state configurations are suggested for the mirror nuclei ^{17}Ne and ^{17}N . A suggested lowering of the $2s_{1/2}$ orbital for the protons is thus consistent with the new shell gap $Z = 16$ reported in Ref. [19]. The present conclusion is also supported by the fact that the lowest resonance for the unbound ^{16}F is a 0^- one showing its s -wave nature, while the 2^- is located above it.

Acknowledgements

The authors are thankful to all cyclotron staff in RRC, RIKEN, for their help in a stable operation of the accelerator.

References

- [1] I. Tanihata, et al., Phys. Rev. Lett. 55 (1985) 2676.
- [2] D. Cortina-Gil, et al., Phys. Lett. B 529 (2002) 36; M.H. Smedberg, et al., Phys. Lett. B 452 (1999) 1; W. Schwab, et al., Z. Phys. A 350 (1995) 283.
- [3] A. Navin, et al., Phys. Rev. Lett. 81 (1998) 5089.
- [4] A. Ozawa, et al., Phys. Lett. B 334 (1994) 18.
- [5] A. Ozawa, et al., J. Phys. G 24 (1998) 143.
- [6] R.E. Warner, et al., Nucl. Phys. A 635 (1998) 292.
- [7] H.T. Fortune, R. Sherr, Phys. Lett. B 503 (2001) 70.
- [8] J.D. Millener, Phys. Rev. C 55 (1997) R1633.
- [9] H. Kitagawa, N. Tajima, H. Sagawa, Z. Phys. A 358 (1997) 381.
- [10] M.V. Zhukov, I.J. Thompson, Phys. Rev. C 52 (1995) 3505.
- [11] L.V. Grigorenko, I.G. Mukha, M.V. Zhukov, Nucl. Phys. A 713 (2003) 372.
- [12] R. Kanungo, et al., Phys. Rev. Lett. 88 (2002) 142502.
- [13] J.A. Tostevin, et al., Phys. Rev. C 66 (2002) 024607.
- [14] G. Bertsch, H. Esbensen, A. Sustich, Phys. Rev. C 42 (1989) 1990; G.F. Bertsch, B.A. Brown, H. Sagawa, Phys. Rev. C 39 (1989) 1154.
- [15] T. Suzuki, et al., Phys. Rev. Lett. 89 (2002) 012501.

- [16] Y. Ogawa, K. Yabana, Y. Suzuki, Nucl. Phys. A 543 (1992) 722.
- [17] H. Ueno, et al., Phys. Rev. C 53 (1996) 2142.
- [18] E. Sauvan, et al., Phys. Lett. B 491 (2000) 1;
- E. Sauvan, Ph.D. Thesis, private communication.
- [19] R. Kanungo, I. Tanihata, A. Ozawa, Phys. Lett. B 528 (2002) 58.